surfaces

MDPI

Article

Eliminating Manifold Pharmaceutical Pollutants with Carbon Nanoparticles Driven via a Short-Duration Ball-Milling Process

Tarig G. Ibrahim [1], Rasmiah S. Almufarij [2,*], Babiker Y. Abdulkhair [1,3,*] and Mohamed E. Abd Elaziz [1]

[1] Department of Chemistry, Faculty of Science, Sudan University of Science and Technology (SUST), P.O. Box 407, Khartoum 13311, Sudan; tariggaffer@gmail.com (T.G.I.); memaziz41@gmail.com (M.E.A.E.)
[2] Department of Chemistry, College of Science, Princess Nourah Bint Abdulrahman University, P.O. Box 84428, Riyadh 11671, Saudi Arabia
[3] Department of Chemistry, College of Science, Imam Mohammad Ibn Saud Islamic University (IMSIU), P.O. Box 90905, Riyadh-KSA, 11623 Riyadh, Saudi Arabia
* Correspondence: rsmufrrig@pnu.edu.sa (R.S.A.); byabdulkhair@imamu.edu.sa or babiker35.by@gmail.com (B.Y.A.)

Abstract: One of the major problems facing humanity in all parts of the world is water pollution. Since carbon nanoparticles (CPs) are known for their excellent absorbability, this study explored preparing CPs via a facilitated ball-milling protocol. Four CP products were prepared with the friction enhancer being variated, typically 0-CPs, 2.5-CPs, 5-CPs, and 10-CPs. The four sorbents were characterized using TEM, EDX, XRD, BET, and FTIR methods. The 0-CPs, 2.5-CPs, 5-CPs, and 10-CPs possessed a BET surface area of 113, 139, 105, and 98.5 m^2 g^{-1}, respectively, and showed a sorption capacity of 55.6, 147.0, 65.8, and 24.6 mg g^{-1} when tested with chlorohexidine (CH). Therefore, the 2.5-CPs were selected as the best sorbents among the prepared nanomaterials and employed for further sorption investigations. The CH sorption on the 2.5-CPs followed the pseudo-second-order, and the liquid–film diffusion controlled the CH sorption onto the 2.5-CPs. The Langmuir isotherm model was followed, and the Dubinin–Radushkevich energy was 3.0 kJ $mole^{-1}$, indicating a physisorption process. The thermodynamic outputs suggested that CH sorption by 2.5-CPs was favorable. Furthermore, the 2.5-CPs sorbent was tested for treating water samples contaminated with 20 mg L^{-1} of ciprofloxacin, dextromethorphan, guaifenesin, metronidazole, ibuprofen, chlorzoxazone, chlorpheniramine malate paracetamol, and hydro-chlorothiazide. The 2.5-CPs showed an average removal efficiency of 94.1% with a removal range of 92.1% to 98.3% and a 2.21 standard deviation value.

Keywords: nonlinear investigation; multidrug removal; water-treatment; Dubinin–Radushkevich; antibiotics; antiseptics

Citation: Ibrahim, T.G.; Almufarij, R.S.; Abdulkhair, B.Y.; Abd Elaziz, M.E. Eliminating Manifold Pharmaceutical Pollutants with Carbon Nanoparticles Driven via a Short-Duration Ball-Milling Process. *Surfaces* **2024**, *7*, 493–507. https://doi.org/10.3390/surfaces7030032

Academic Editors: Gaetano Granozzi and Mohamed M. Chehimi

Received: 21 May 2024
Revised: 12 July 2024
Accepted: 16 July 2024
Published: 18 July 2024

1. Introduction

Surface water and groundwater resources play a significant role in agriculture, livestock production, industrial activities, forestry, fisheries, and recreational activities [1,2]. Water is considered polluted when some quality parameter is hampered, usually by unguided and irregulated anthropogenic activities [3]. Pharmaceutical contaminants (PCs) were first identified in the United States and Europe surface water in the 1960s and were recognized as a concern in 1999, giving pollution a 40-year head start [4]. The pharmaceutical compounds are essential for medication and agricultural productivity, and their demands continue to grow [5]. The sources of contamination include hospitals, landfills, runoff from agricultural fields, urban waste, city street wash, cultivated fields, and even graveyards [6,7]. Factory locations are often near rivers and the seashore because manufacturing processes require water, and sadly, companies contaminate water supplies with their wastes [8]. Such industrial wastewater may contain organic solvents, intermediates, and raw materials, which are challenging to treat [9]. After the partial metabolism of drugs, secretion into urine and feces leads them to wastewater and eventually to water

bodies. The literature survey revealed the globality of PCs occurrence in several large water bodies worldwide, such as the Red Sea [10], China's marine water [11], and several rivers in Europe [12,13]. Such toxic substances in water lower the chemical oxygen demand, disrupt ecological life, and threaten human health [14,15]. The presence of antibiotics and antiseptics in water is among the most concerning problems since they cause endocrine disruption and develop drug-resistant bacteria; it was also accused of feminizing fish living downstream of wastewater treatment plant outfalls. Also, a link between anti-inflammatory medicines and renal failure has been reported [16,17]. Analgesic, antipyretic, antibiotic, and antiseptic drugs are among the most excessively used medications [18]; therefore, they will be used as example pollutants in this study. Diverse water treatment methods have been used to provide uncontaminated water supplies. Conventional water treatment (CWT) focuses on removing microorganisms and reducing the dissolved ions in water to meet drinking water standards; the treatment process uses the best affordable technologies for local raw water characteristics. One CWT comprises a coagulation process that involves converting small particles into larger aggregates, followed by subsequent solid/liquid separation [19]. The coagulation procedure may require electrical neutralization by oppositely charged metal ions to yield an organic–ion insoluble complex [20]. Another common CWT is sedimentation, which is employed to reduce the suspended particles in water by gravity settlement before or sometimes after coagulation. The prementioned CWT is usually followed by filtration to remove suspended solids via a bed packed with granular media. Filtration focuses mainly on turbidity [21,22]. Slow sand filtration was historically the first to be employed, while rapid sand filtration was later favored because of the insufficient output of the first [23]. Although conventional treatment processes are used, many studies have revealed the occurrence of PCs in drinking water in Spain, China, England, and the United States [24]. As conventional water-treatment methods failed to remove PCs effectively from water resources, adsorption methods are of great interest these days [25]. Many forces may bind contaminants to the sorbent's surface, such as hydrogen bonding, π–π bonding, induced dipole interaction, and van der Waals forces [26]. The sorbate's polarity, adsorbent's pore size, surface area, and functional groups can affect the removal efficiency. Although the adsorption process requires an additional treatment of adsorbed material after removal from water, it requires no light source and produces no carcinogenic radicals or toxic products. Since the expansion of nanoscience, the production of sorbents with high surface area has positively affected the applicability and effectiveness of the adsorption process. The removal of PCs from water was studied using metal oxide nanoparticles, nanocomposites, and carbonaceous materials (CMs) [27–29]. In addition, the feasibility, safety, high surface area, and excellent adsorbing properties nominated the CMs allotropes as potential water treatment substrates [30,31]. CMs superseded metal oxides because the first could be produced from various commercially available precursors, biomass waste substrates, and industrial waste. Converting such waste into a usable substance is advantageous and a potential solution to an environmental issue [32–37].

Among the CMs, carbon nanoparticles (CPs) were known for their high surface area by which the adsorption capacity may increase significantly. CPs are porous materials with a variety of tiny pores of varying sizes. The main techniques for large-scale production include the wet chemical process during which CMS or its precursor is subjected to oxidizing agents such as protonated solvents. This procedure forms a covalent bond between carboxyl and hydroxyl groups and CPs. Additionally, the ball-milling protocol is a process that downsizes CMs to obtain CPs. Wet ball milling utilizes solvents, such as ethanol, toluene, and chloroform, to enhance the milling process's efficiency. When solvents were added to the ball-milling process, it was found that this method had clear advantages over the standard dry-milling procedure, such as achieving a more uniform size distribution [15,38–40]. Perhaps due to the difficulty of removing solid additives, researchers avoided using solid solvents, even though they are more beneficial to grinding processes than liquid solvents. Our vision is that this matter can be avoided by using solids

dissolved in water, which are later disposed of by washing with a sufficient amount of appropriate solvent.

Because of the superiority of carbon adsorbents over metal oxide sorbents in treating extremely acidic and/or highly alkaline industrial effluents, CPs will be prepared as feasibly applicable adsorbents. The CPs will be generated from an inexpensive starting material employing an easy method and readily available equipment, namely ball milling. This study aims to investigate the effectiveness of sucrose as a friction facilitator instead of a liquid solvent. The prepared CPs will be studied for purifying water from manifold PCs, such as ciprofloxacin (CIP), dextromethorphan (DEX), guaifenesin (GUA), metronidazole (MET), ibuprofen (IBU), chlorzoxazone (CHL), chlorpheniramine malate (CFM), paracetamol (PAR), hydrochlorothiazide (HCT), and chlorohexidine (CH).

2. Experimental

2.1. Materials

Sodium hydroxide (NaOH) and hydrochloric acid (HCl, 37%) were obtained from Sigma Aldrich, Miami, FL, USA. Commercial ethanol (EtOH, 95%), sucrose (Su), and commercial charcoal (Cch) were obtained from the local market. Working standards of CIP, DEX, GUA, MET, IBU, CHL, CFM, PAR, HCT, and CH, were obtained from Rhanboxy, Mumbai, India.

2.2. CPs Preparations

The Su was employed as a soluble milling facilitator to prepare the CPs. The Cch and mixtures of Cch with 2.5% Su, 5% Su, and 10% Su were milled in a 60 mL stainless steel crucible with 5 stainless steel balls (1.0 cm diameter). The machine (Ball- mill, Netzspannungswashi, 07.4000/01343, Selb, Germany) was operated for 5.0 h, utilizing the reverse mode at 600 RPM, and the milling products were labeled 0-CPs, 2.5-CPs, 5-CPs, and 10-CPs. A total of 100 mL of distilled water (DW) was added to each of the four products in a separate beaker, sonicated for 20 min in an ultrasonic bath, filtered, rinsed with distilled water, and dried at 110 °C for 3.0 h.

2.3. Characterization of CPs

An analysis was performed on the 0-CPs, 2.5-CPs, 5-CPs, and 10-CPs using a Fourier-transform infrared-spectrophotometer (FTIR-Tracer-100, Shimadzu, Tokyo, Japan), energy dispersive x-rays (EDX, JSM-IT500, Miami, FL, USA), a transmission electron microscope (JEM-1400-Flash, Jeol, Miami, FL, USA), a powder X-ray diffractometer (XRD-Bruker-D8 Advance, Billerica, Miami, FL, USA), and a surface analyzer (Micromeritics ASAP-2020, Miami, FL, USA).

2.4. Adsorption Studies

The sorption capabilities of 0-CPs, 2.5-CPs, 5-CPs, and 10-CPs were inspected utilizing CH as a pollutant model. Typically, 50 mg of each was stirred with 150 mL of 100 mg L^{-1} CH solution, and an aliquot was picked and filtered via a membrane filter. Then, the pollutant's absorbance was measured at selected time intervals using a Shimadzu UV-Vis spectrophotometer set at 260 nm [41,42]. The pH influence on the sorption process was inspected from pH 2.0 to 10.0, and the pollutant solutions were adjusted utilizing 0.2MHCl and the NaOH solutions, and a portion of each adjusted solution was utilized as standard for its own sample. The effect of concentration on the sorption was investigated at 20 °C utilizing CH concentrations from 25 to 100 mg L^{-1}. The aforementioned concentrations were employed to study the temperature influence at 20 °C, 35 °C, and 50 °C. A 20 mg L^{-1} solution of each drug was prepared, and 150 mL of each solution was stirred separately with 50 mg of the 2.5-CPs for 1.0 h, then filtered. The absorbances were measured via the UV-Vis spectrophotometer using the comparative evaluation method. The adsorption capacity (q_t, (mg g^{-1})) was computed (Equation (1)) using the solution volume (v, (L)),

the sorbent mass (m, (g)), while the pollutant concentrations at t = 0 and t = t (min) were denoted as C_o and C_t.

$$q_t = \frac{(C_o - C_t)V}{m} \quad (1)$$

3. Results and Discussion

3.1. Characterization

Figure 1a–d illustrate the TEM images exposing the surface morphology of 0-CPs, 2.5-CPs, 5-CPs, and 10-CPs. The results showed particle size ranges of (30.9–136.0 nm), (16.2–32.8 nm) (10.4–43.9 nm), and (32.2–58.5 nm), respectively. The images unraveled the effectiveness of using the water-soluble milling facilitator to enhance the production of uniform-sized CPs using the ball-milling protocol. It appeared that the 2.5% Su was the best amount of the studied Su amounts, followed by the 5% Su, while increasing the enhancer ratio to ≥10% may lower its milling facilitation, which can be attributed to the agglomeration of sucrose together when occurring at a high amount. In addition, the EDX was utilized to examine the elemental composition of 0-CPs, 2.5-CPs, 5-CPs, and 10-CPs (Figure 2). The results revealed that the sample constituted mainly carbon and trace calcium, which might be from the original tree source of the charcoal and/or the commercial carbonization process.

The N_2-adsorption–desorption isotherm was utilized to investigate the pore shapes, specific pore volume (SPV), surface area (SA), and average pore diameter (APD) [43]. Figure 3a–d monitored the produced hysteresis loops and the SPV distributions for the 0-CPs, 2.5-CPs, 5-CPs, and 10-CPs. Notably, the 0-CPs, 5-CPs, and 10-CPs illustrated a hysteresis loop of type H4 associated with slit-like, micro-mesoporous sorbents of aggregated crystals that formed. On the other hand, the 2.5-CPs resulted in a hysteresis H3 loop associated with non-rigid aggregated sorbents with wedge-shaped, mesoporous, plate-like particles. This variation of hysteresis loops and pore shapes might be the perk that caused the increased 2.5-CPs total surface (Table 1) [44–47].

Table 1. The surface characteristics of as-prepared 0-CPs, 2.5-CPs, 5-CPs, and 10-CPs.

Sorbent	SA ($m^2\ g^{-1}$)	APD (Å)	SPV ($cm^3\ g^{-1}$)
0-CPs	113	11.268	0.335
2.5-CPs	139	11.446	0.363
5-CPs	105	9.500	0.332
10-CPs	98.5	8.280	0.220

The XRD diffractometer was employed to investigate the crystallinity-phase purity of the 0-CPs, 2.5-CPs, 5-CPs, and 10-CPs. Figure 4a demonstrates the XRD diffraction outputs of the 0-CPs, 2.5-CPs, 5-CPs, and 10-CPs. The diffraction peaks around 2θ° of 26.84 and 43.28, attributed to the planes of the lattice phases (002) and (100) of the crystalline carbon (JCPDS no. 04-0850) [47,48]. The EDX outputs of minor metal oxide in Cch can explain the XRD spectrum's extra peaks.

Additionally, the functional groups of synthesized 0-CPs, 2.5-CPs, 5-CPs, and 10-CPs were inspected employing FTIR (Figure 4b). The bands ranging between 400 and 900 cm^{-1} can be allocated to the metal oxides announced by EDX and XRD. The 1429 and 1590 cm^{-1} peaks can be allocated to the C-C, C=C, while the 1708 cm^{-1} can be interpreted as a C≡C of terminal carbon skeletons and/or a carbonyl group. Furthermore, a slight inflation can be seen above 3000 cm^{-1}, indicating an acidic OH group.

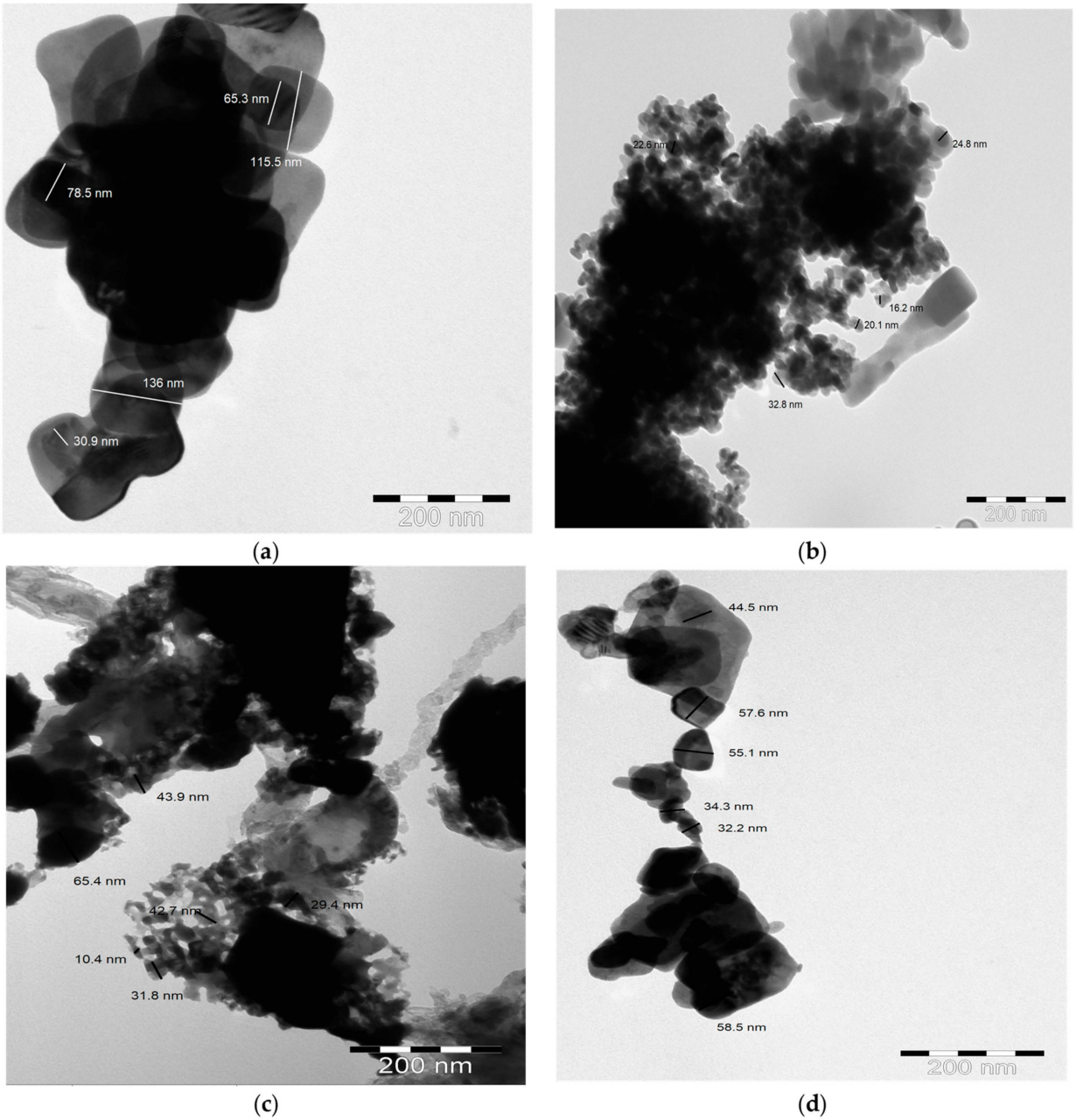

Figure 1. (**a**–**d**) TEM images of 0-CPs, 2.5-CPs, 5-CPs, and 10-CPs, respectively.

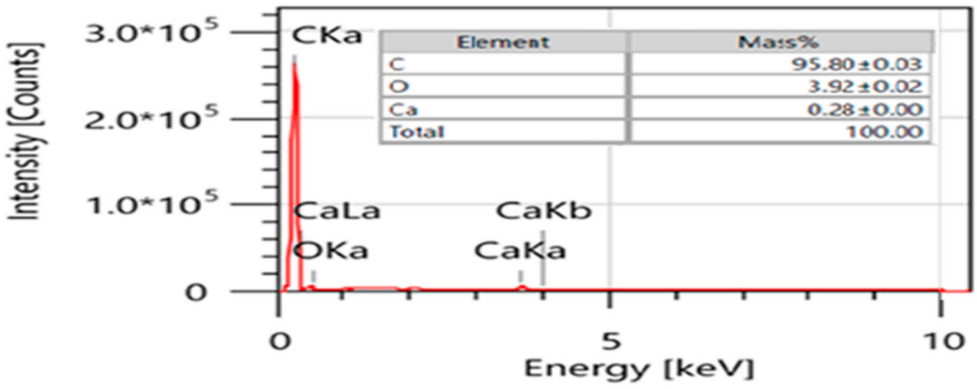

Figure 2. EDX results of the fabricated 2.5-CPs.

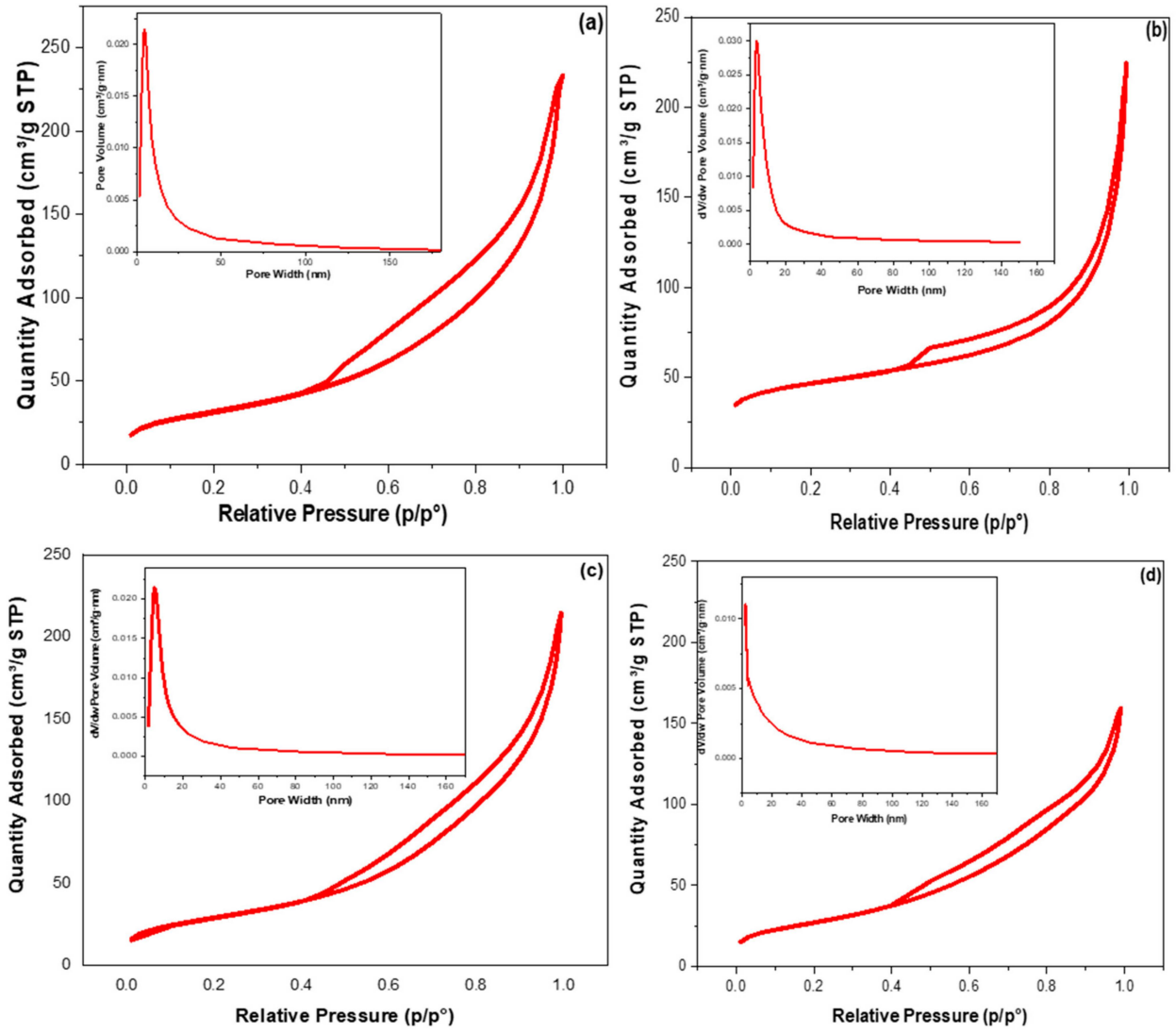

Figure 3. N_2- adsorption–desorption isotherm and pore size distribution of (**a**) 0-CPs, (**b**) 2.5-CPs, (**c**) 5-CPs, and (**d**) 10-CPs.

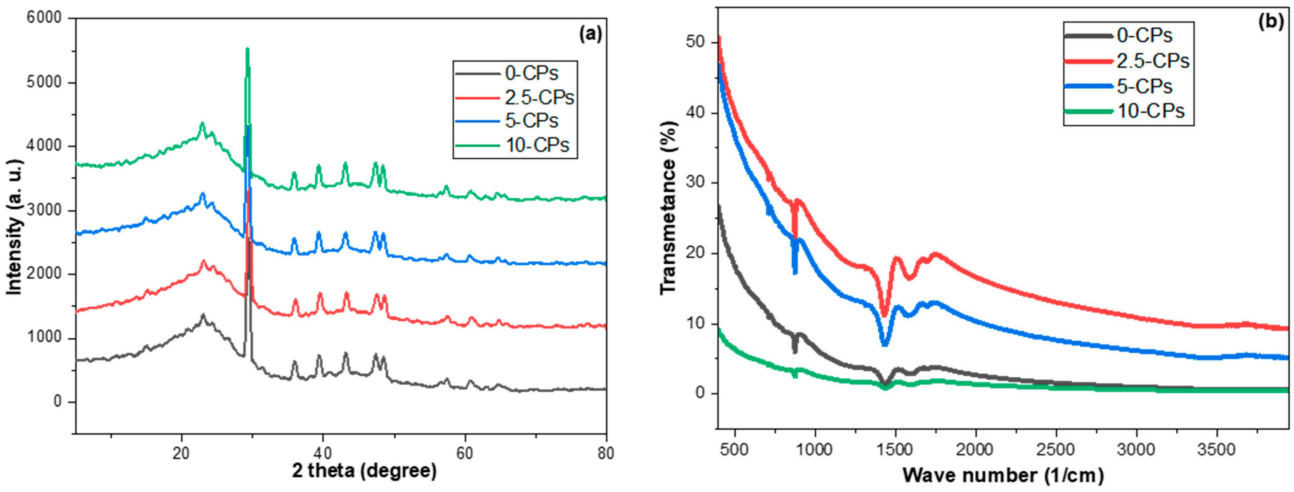

Figure 4. (**a**) XRD pattern and (**b**) the FTIR results of 0-CPs, 2.5-CPs, 5-CPs, and 10-CPs.

3.2. Adsorption Investigations

Figure 5a illustrates the contact time investigations of CH sorption onto the 0-CPs, 2.5-CPs, 5-CPs, and 10-CPs studied. It took 90 min to attain equilibrium, with qt values of 55.6, 147.0, 65.8, and 24.6 mg g^{-1}. These findings suggest that including sucrose in the Cch improves grinding; however, the amount of sugar is critical in determining the milling efficacy. Adding sucrose as a milling facilitator possessed a positive impact on the milling process with a sucrose percentage of up to 5%; since the 2.5-CPs was the best across the tested range, its sorption was further investigated. Figure 5b demonstrates the impact of CH concentration on adsorption. Elevating starting concentrations produces a potent CH movement toward 2.5-CPs, and the line inflation between 75 and 100 mg L^{-1} indicated the suitability of 1.0 g to treat 3.0 L of water polluted by up to 75 mg L^{-1} CH. These outcomes may nominate 2.5-CPs for efficient industrial wastewater treatment. Moreover, the temperature impact on CH removal by 2.5-CPs was studied. The proportional decrease in q_t as the heat was raised suggested exothermic sorption (Figure 5b). Because it affects the availability and accessibility of functional groups on the sorbent's surface and pollutant molecules, the impact of pH was studied [49]. Figure 5c illustrates a significant decrease in q_t values below pH 4.0 and above pH 8.0, attributed to protonating the CH and 2.5-CPs electron-rich sites and the $^{-}$OH ion–CH competition, respectively [50].

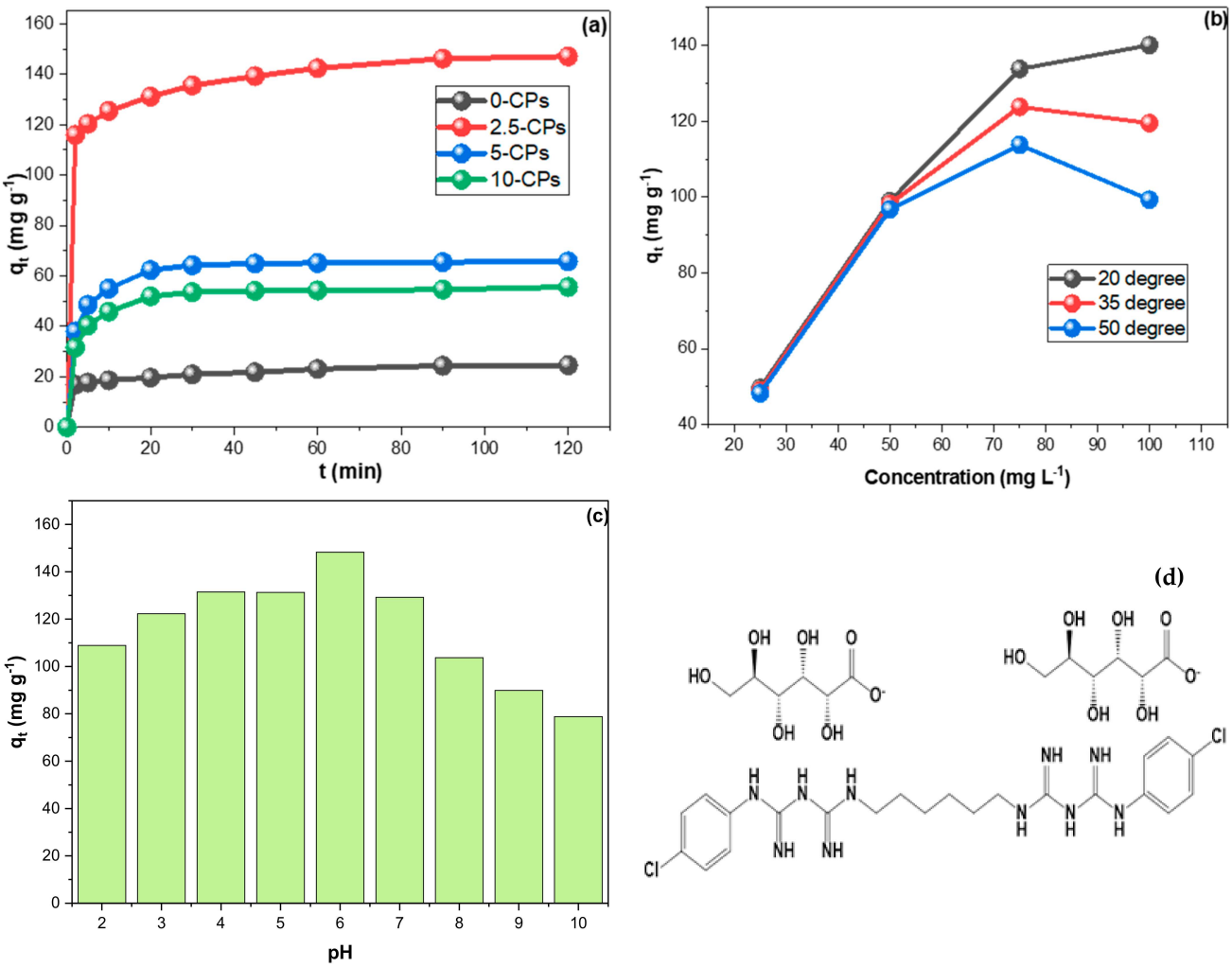

Figure 5. (**a**) Contact time impact on CH removal by 50 mg of 0-CPs, 2.5-CPs, 5-CPs, and 10-CPs from 150 mL of 100 mgL^{-1} solution, (**b**) effect of CH concentration on the sorption process, (**c**) impact of solution pH on the CH sorption onto 2.5-CPs, and (**d**) CH structure.

3.3. Kinetics

The kinetic of CH sorption onto the 2.5-CPs was assessed using the nonlinear pseudo-first-order (PFO) and the nonlinear pseudo-second-order (PSO) Equations (2) and (3), respectively. The mechanism controlling the sorption was examined via the liquid film (LFM, Equation (4)) and intraparticle-diffusion models (IPM, Equation (5)) [51,52].

$$q_t = q_e\left(1 - \exp^{-K_1 \cdot t}\right) \quad (2)$$

$$q_t = \frac{k_2.q_e^2.t}{1 + k_2.q_e.t} \quad (3)$$

$$q_t = K_{IP} * t^{\frac{1}{2}} + C_i \quad (4)$$

$$\ln(1 - F) = -K_{LF} * t \quad (5)$$

where k_1 (min^{-1}), k_2 (g mg^{-1} min^{-1}), k_{IP} (mg g^{-1} $min^{-1/2}$), and k_{LF} (min^{-1}) represent PFO, PSO, IPM, and LFM constants, respectively. C_i is the IPM boundary layer factor [53]. The linear regression plots of the four models are illustrated in Figure 6, and their findings are collected in Table 2. The CH sorption onto 2.5-CPs showed a higher R^2 value with the PSO model and a lower reduced chi-square magnitude than that of PFO. Additionally, the adsorption mechanism investigations showed almost equal R^2 values indicating that LFD and IPD both participated in controlling the CH sorption onto the 2.5-CPs [29].

Table 2. The kinetics, isotherms, and thermodynamic results of CH sorption onto 2.5-CPs.

Kinetics									
Adsorption rate order									
q_e experimental. (mg g^{-1})	PFO				PSO				
	qe cal. (mg g^{-1})	R^2 (au)	k_1 (min^{-1})		qe cal. (mg g^{-1})		R^2 (au)	k_2 (g mg^{-1} min^{-1})	
147.042	132.364	0.952	0.983		71.449		0.973	0.027	
Adsorption rate control mechanism									
IPM					LFM				
K_{IP} (mg g^{-1} $min^{0.5}$)	C (mg g^{-1})		R^2		K_{LF} (min^{-1})		R^2		
4.192	11.291		0.8129		0.0496		0.8645		
Isotherms									
Langmuir			Freundlich			Dubinin–Radushkevich			
R^2	K_L (L mg^{-1})	q_m (mg g^{-1})	R^2	K_f (L mg^{-1})	n^{-1} (a.u.)	R^2	qm (mg g^{-1})	K_D (mol^2 J^{-1})	E (kJ mol^{-1})
0.987	0.026	140.902	0.829	90.194	6.781	0.929	147.567	0.056	3.000
Thermodynamics									
Fed conc. (mg L^{-1})	ΔH° (kJ mol^{-1})		ΔS° (kJ mol^{-1})		ΔG° (kJ mol^{-1}) 298 K		ΔG° (kJ mol^{-1}) 313 K		ΔG° (kJ mol^{-1}) 328 K
25	−44.614		−0.109		−12.016		−10.375		−8.734
50	−30.274		−0.063		−11.355		−10.402		−9.450
75	−26.178		−0.070		−5.230		−4.176		−3.122
100	−23.289		−0.071		−2.132		−1.067		−0.002

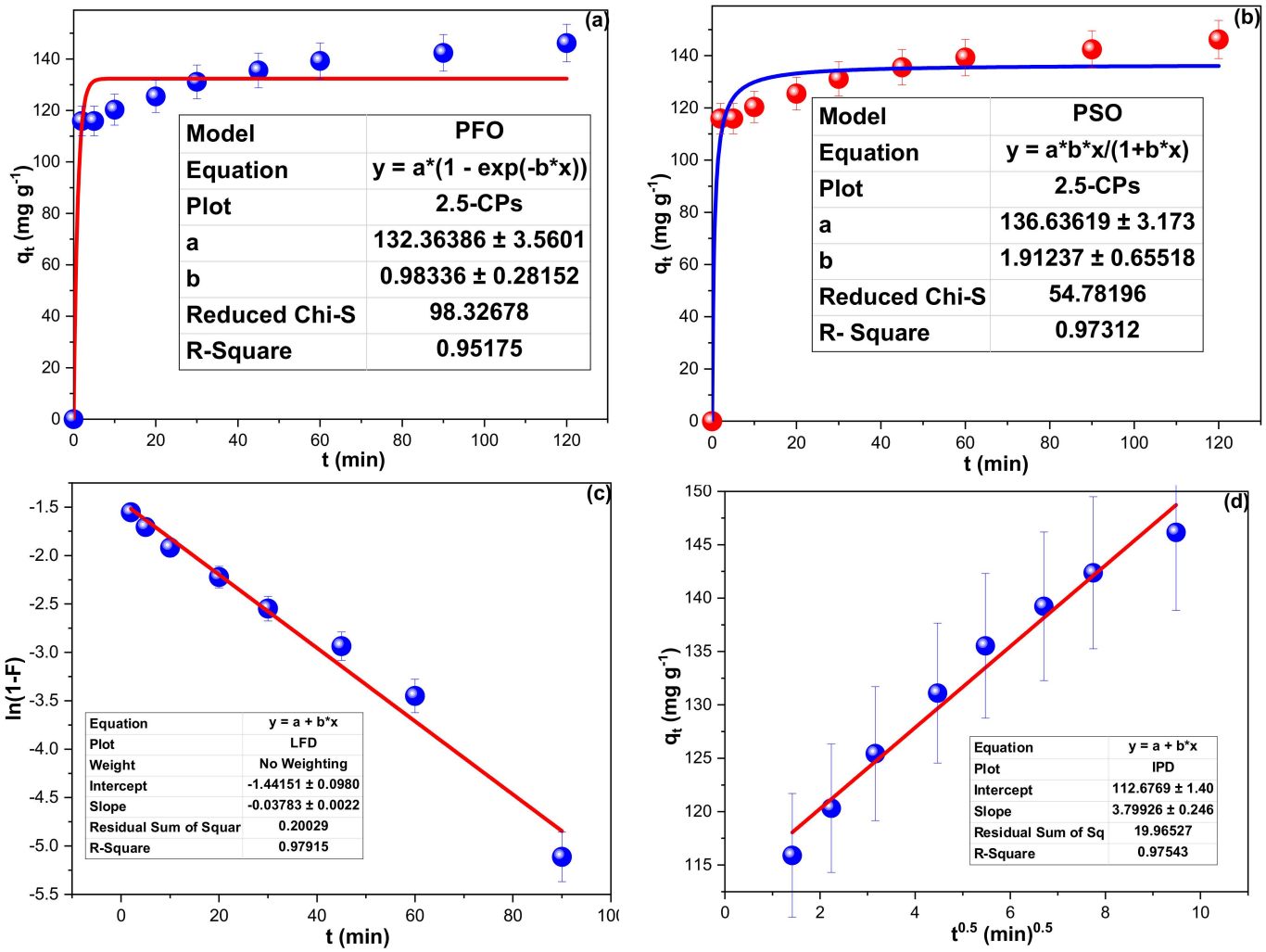

Figure 6. (**a**) PFO, (**b**) PSO, (**c**) IPM, and (**d**) LFM investigations of CH sorption onto 2.5-CPs.

3.4. Isotherms

The results of CH sorption from 25, 50, 75, and 100 mg L^{-1} concentrations were employed to investigate the sorption isotherm on the 2.5-CPs [46,54]. The adsorption isotherms have been described using the Langmuir (LIM; Equation (6)) for the mono-layered pattern and Freundlich (FIM; Equation (7)) for the multi-layered pattern. The Dubinin–Radushkevich model (DRM, Equation (8)) was utilized to better understand the sorption process.

$$q_e = \frac{K_l q_m C_e}{1 + q_m C_e} \quad (6)$$

$$q_e = K_F . C_e^{\frac{1}{n}} \quad (7)$$

$$\ln q_e = \ln q_m - K_D \varepsilon^2 \quad (8)$$

Langmuir and Freundlich's constants are represented by (K_L, L mg^{-1}) and (K_F, L mg^{-1}); qm (mg g^{-1}) is the computed maximum q_t, and the Freundlich-heterogeneity factor was noted as (n). The Dubinin energy (E_D, kJ $mole^{-1}$) and the Polanyi's potential (ε, kJ mol^{-1}) were computed via Equations (9) and (10), respectively, and the Dubinin constant K_D (kJ^2 mol^{-2}) was calculated using the slope value.

$$\varepsilon = RTln\left(1 + \frac{1}{C_e}\right) \quad (9)$$

$$E_D = (2K_D)^{-0.5} \quad (10)$$

Table 2 shows the computed values for LIM, FIM, and DRM according to their plots in Figure 7. The CH adsorption onto 2.5-CPs fitted the LIM with higher R^2 and lower reduced Chi-square values, and the unfavorability of multilayer-sorption has been revealed by the low R^2 and high 1/n values [55]. The E_D value of 3.0 kJ mole^{-1} (less than 9.0) indicated that CH elimination by the 2.5-CPs and was performed via a physisorption process [6].

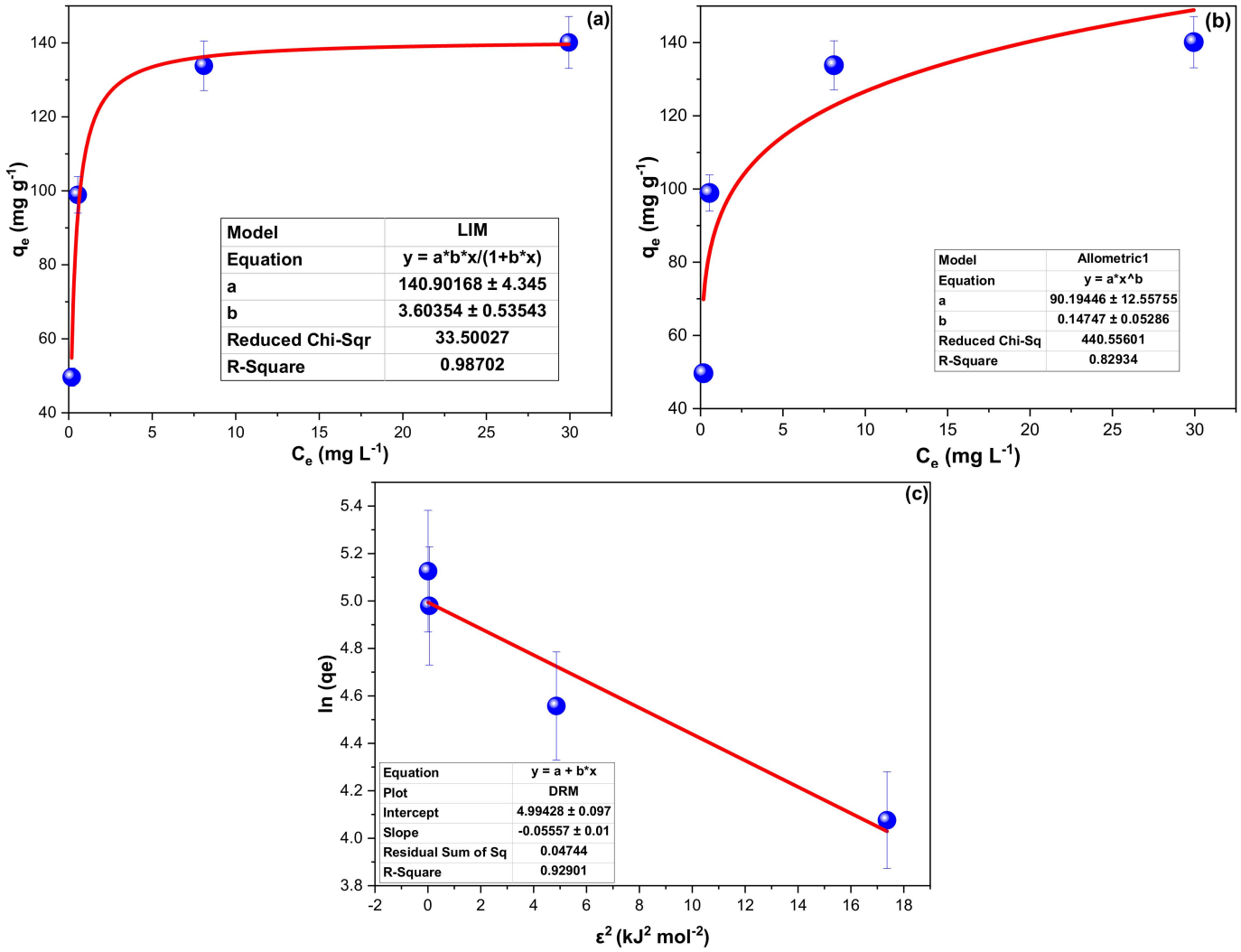

Figure 7. (**a**) LIM (**b**) FIM, and DRM plots of CH adsorption onto the 2.5-CPs.

3.5. Thermodynamics

In order to learn more about how CH adsorbs onto the engineered 2.5-CPs, the underlying thermodynamics were investigated. Equation (11) related the enthalpy and entropy, symbolled as ΔH^o and ΔS^o, which were computed from the slope and intercept from plotting (ln(Kc)) versus (1/T (K^{-1})) (Figure 8). Furthermore, the makeup of ΔH^o and ΔS^o alongside the temperature (K) in Equation (12) generated the Gibbs free-energy (ΔG^o) values (Table 2).

$$\ln K_c = \frac{\Delta H^o}{RT} + \frac{\Delta S^o}{R} \quad (11)$$

$$\Delta G^{o} = \Delta H^{o} - T\Delta S^{o} \quad (12)$$

where Kc was calculated by dividing the adsorbed CH concentration by its concentration in the solution. The negative ΔH^{o} values defined CH removal by 2.5-CPs as exothermic sorption. Furthermore, the negative values of ΔG^{o} implied the spontaneity of CH adsorption within the concentration and temperature ranges of 25 to 100 mgL^{-1} and 20 to 50 °C, respectively. Additionally, the acquired ΔG^{o} values demonstrated that an increase in the temperature of the solution led to a reduction in the spontaneity of CH elimination. In addition, the data concerning ΔS^{o} were negative, which suggested favorable CH adsorption onto 2.5-CPs [56].

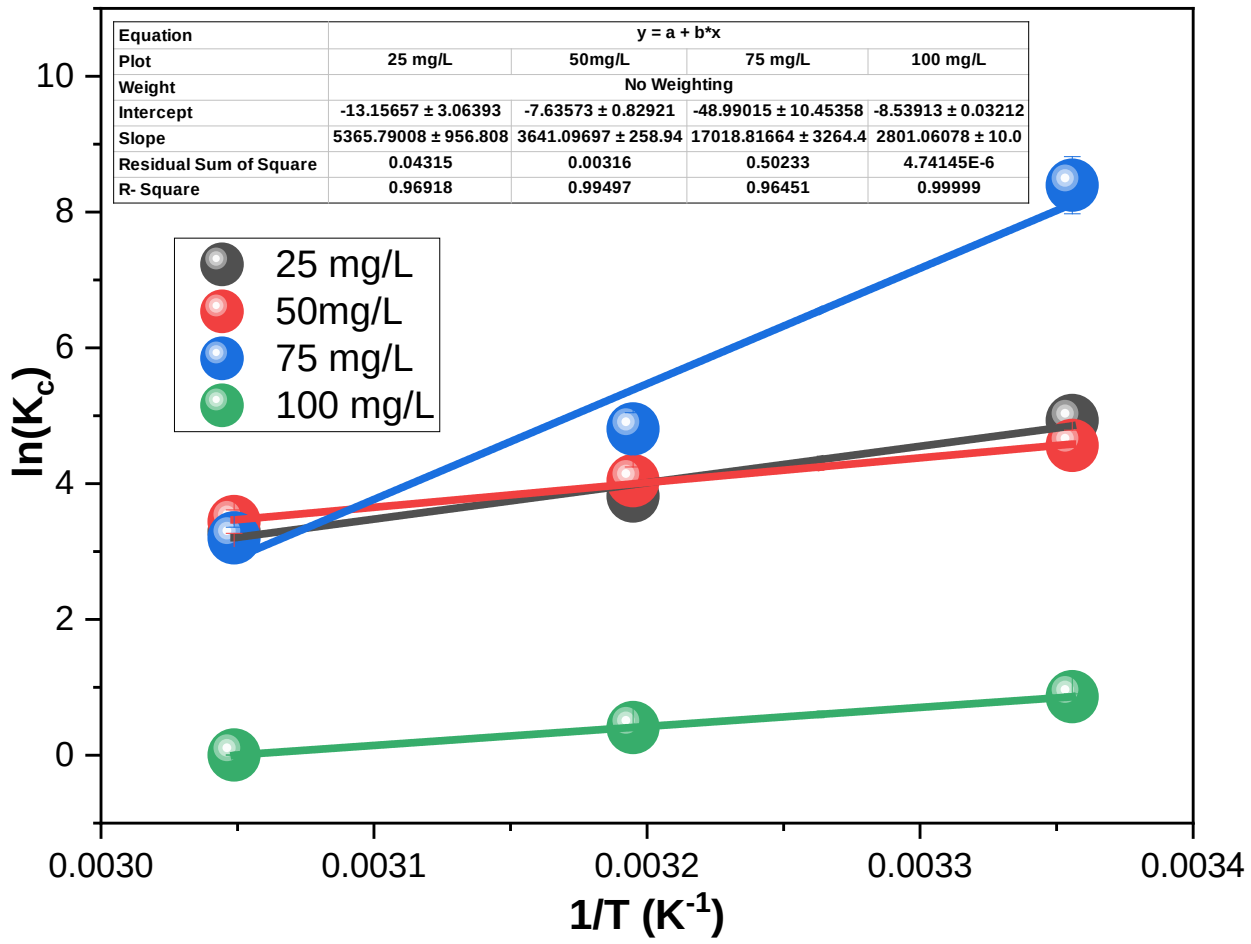

Figure 8. Thermodynamic plots of CH adsorption onto 2.5-CPs from 25, 50, 75, and 100 mg L^{-1} concentrations at 298 to 328 K^{-1}.

3.6. Application to Other Pharmaceutical Pollutants

Figure 9 shows the chemical structure of CIP, DEX, GUA, MET, IBU, CH, CFM, PAR, and HCT. As can be seen, all the ten PCs are rich with π electrons which indicates the possibility of π–π interaction between the 2.5-CPs and pollutants. The CIP, DEX, GUA, MET, IBU, CH, CFM, PAR, and HCT were measured at a wavelength of 276, 228, 230, 325, 224, 260, 225, 240, and 228 nm, respectively, and the performance of 2.5-CPs is illustrated in Figure 10. The prepared 2.5-CPs showed an average removal efficiency of 92.9% with a removal range of 88.2 to 98.3% and an RSD of 3.3%. These results indicated the applicability of the 2.5-CPs as an effective sorbent for treating industrial waste effluents with manifold pharmaceutical pollution, such as the wastewater of pharmaceutical companies.

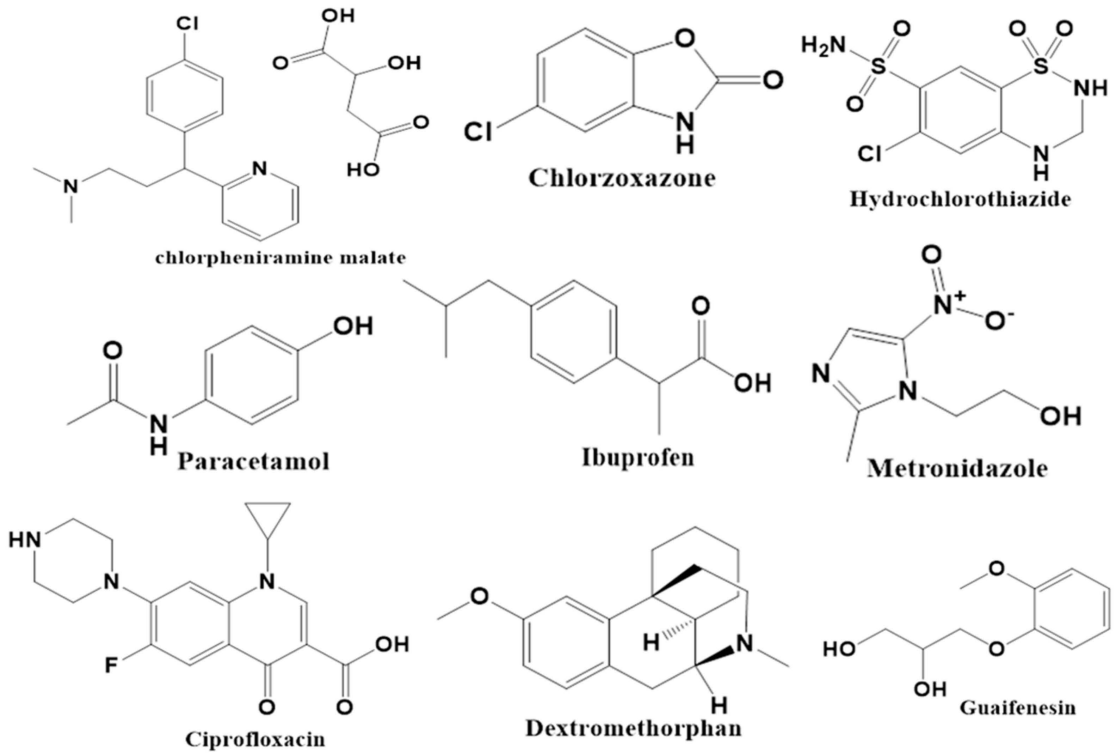

Figure 9. The chemical structure of the antiseptic and antibiotics employed as pollutant examples for manifold pharmaceutical pollutants treatment.

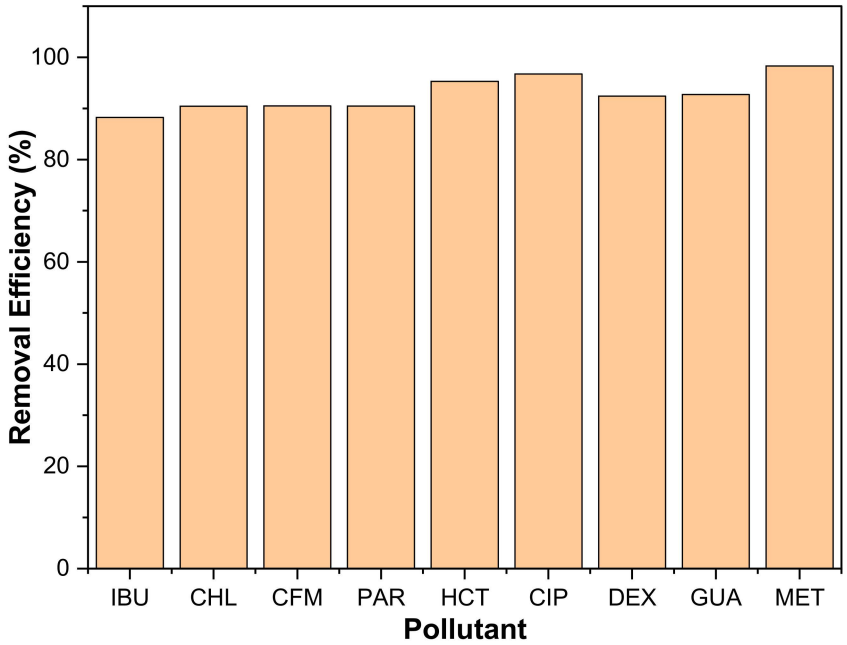

Figure 10. The 2.5-CPs efficiency in adsorbing CIP, DEX, GUA, MET, IBU, CHL, CFM, PAR, and HCT by mixing 50 mg sorbent with 150 mL of the 20 mgL^{-1} drug solution.

4. Conclusions

Sucrose is employed as a water-soluble milling facilitator to fabricate the 0-CPs, 2.5-CPs, 5-CPs, and 10-CPs. The TEM finding of the 0-CPs, 2.5-CPs, 5-CPs, and 10-CPs exposed the particle size within the nanoscale, with a preference for the 2.5% milling facilitator. The XRD diffractometer revealed diffraction peaks of 23.84 and 43.28 2θ° that

attributed to the (002) and (100) planes of crystalized graphite. Furthermore, the FTIR detected weak bands above 3000 cm^{-1}, indicating a hydroxyl group. The N_2 isotherm analysis prevailed in a surface area of 113, 139, 105, and 98.5 m^2 g^{-1} for the 0-CPs, 2.5-CPs, 5-CPs, and 10-CPs. The contact time study for CH elimination by the 0-CPs, 2.5-CPs, 5-CPs, and 10-CPs took about 90 min to attain equilibrium and showed q_t values of 55.6, 147.0, 65.8, and 24.6 mg g^{-1}. These findings aligned with the surface analysis; hence, 2.5-CPs were selected for further studies. The removal of CH was better at a pH value of 6.0, and its q_t values decreased significantly in the strongly acidic and basic mediums. The CH sorption onto 2.5-CPs followed the PFO model, and LFM was the slowest sorption step, indicating that CH was spontaneously attracted toward the 2.5-CPs. Also, the CH adsorption onto 2.5-CPs followed the LIM, and the unfavorability of multilayer sorption was reflected in the Freundlich boundary layer factor. The acquired ΔG° values demonstrated spontaneous CH sorption onto 2.5-CPs at low temperatures. The 2.5-CPs were tested for removing CIP, DEX, GUA, MET, IBU, CH, CFM, PAR, and HCT from water and showed an average removal efficiency of 92.9% with a removal range of 88.2 to 98.3% and an RSD of 3.3%. The results demonstrated that the 2.5-CPs could be nominated to remove pharmaceutical pollutants from industrial pharmaceutical waste effluents effectively.

Author Contributions: Conceptualization, B.Y.A. and M.E.A.E.; methodology, T.G.I. and R.S.A.; software, R.S.A.; validation, and formal analysis, T.G.I.; investigation, B.Y.A.; resources, R.S.A.; data curation, T.G.I.; writing—original draft preparation, T.G.I. and R.S.A.; writing—review and editing, B.Y.A.; visualization, supervision, and project administration, M.E.A.E.; funding acquisition, R.S.A. All authors have read and agreed to the published version of the manuscript.

Funding: Princess Nourah bint Abdulrahman University Researchers Supporting Project number (PNURSP2024R316), Princess Nourah bint Abdulrahman University, Riyadh, Saudi Arabia.

Institutional Review Board Statement: Not applicable.

Data Availability Statement: Data will be made available on request.

Acknowledgments: The authors would like to thank Princess Nourah bint Abdulrahman University for the Researcher's Supporting Projects.

Conflicts of Interest: The authors declare that they have no known competing financial interests or personal relationships that could have appeared to influence the work reported in this paper.

References

1. Narasimhan, T.N. A note on India's water budget and evapotranspiration. *J. Earth Syst. Sci.* **2008**, *117*, 237–240. [CrossRef]
2. Priyadarshi, H.; Singh, R.D.; Sharma, K.D. India's Water Resources Management—Difficulties and Opportunities. *Curr. Sci.* **2005**, *89*, 794–811.
3. Hamid, S.; Yaseen, A.; Kamili, A.N.; Yatoo, A.M. Pollution in Aquatic Environs: Sources and Consequences. In *Bioremediation and Biotechnology*; Springer: Berlin/Heidelberg, Germany, 2020; Volume 4, pp. 21–38.
4. Daughton, C.G.; Ternes, T.A. Pharmaceuticals and personal care products in the environment: Agents of subtle change? *Environ. Health Perspect.* **1999**, *107* (Suppl. S6), 907–938. [CrossRef] [PubMed]
5. Sayadi, M.H.; Trivedy, R.; Pathak, R.K. Pollution of pharmaceuticals in environment. *J. Ind. Pollut. Control.* **2010**, *26*, 89–94.
6. Almufarij, R.S.; Abdulkhair, B.Y.; Salih, M. Fast-simplistic fabrication of MoO_3@Al_2O_3-MgO triple nanocomposites for efficient elimination of pharmaceutical contaminants. *Results Chem.* **2024**, *7*, 101281. [CrossRef]
7. Khetan, S.K.; Collins, T.J. Human pharmaceuticals in the aquatic environment: A challenge to green chemistry. *Chem. Rev.* **2007**, *107*, 2319–2364. [CrossRef] [PubMed]
8. Khatun, R. Water pollution: Causes, consequences, prevention method and role of wbphed with special reference from Murshidabad district. *Int. J. Sci. Res. Publ.* **2017**, *8*, 269–277.
9. Sreekanth, D.; Sivaramakrishna, D.; Himabindu, V.; Anjaneyulu, Y. Thermophilic treatment of bulk drug pharmaceutical industrial wastewaters by using hybrid up flow anaerobic sludge blanket reactor. *Bioresour. Technol.* **2009**, *100*, 2534–2539. [CrossRef] [PubMed]
10. Ali, A.M.; Rønning, H.T.; Alarif, W.; Kallenborn, R.; Al-Lihaibi, S.S. Occurrence of pharmaceuticals and personal care products in effluent-dominated Saudi Arabian coastal waters of the Red Sea. *Chemosphere* **2017**, *175*, 505–513. [CrossRef] [PubMed]
11. Tsui, M.M.; Leung, H.W.; Wai, T.C.; Yamashita, N.; Taniyasu, S.; Liu, W.; Lam, P.K.; Murphy, M.B. Occurrence, distribution and ecological risk assessment of multiple classes of UV filters in surface waters from different countries. *Water Res.* **2014**, *67*, 55–65. [CrossRef] [PubMed]

12. Nannou, C.I.; Kosma, C.I.; Albanis, T.A. Occurrence of pharmaceuticals in surface waters: Analytical method development and environmental risk assessment. *Int. J. Environ. Anal. Chem.* **2015**, *95*, 1242–1262. [CrossRef]
13. Paíga, P.; Santos, L.H.; Ramos, S.; Jorge, S.; Silva, J.G.; Delerue-Matos, C. Presence of pharmaceuticals in the Lis river (Portugal): Sources, fate and seasonal variation. *Sci. Total Environ.* **2016**, *573*, 164–177. [CrossRef] [PubMed]
14. Chelliapan, S. *Treatment of Pharmaceutical Wastewater Containing Macrolide Antibiotics by Up-Flow Anaerobic Stage Reactor (UASR)*; University of Newcastle upon Tyne: Newcastle upon Tyne, UK, 2006.
15. Wu, J.; Wang, T.; Li, S.; Tang, W.; Yu, S.; Zhao, Z.; Chen, J. A green method to improve adsorption capacity of hydrochar by ball-milling: Enhanced norfloxacin adsorption performance and mechanistic insight. *Carbon Res.* **2024**, *3*, 60. [CrossRef]
16. Larsson, S.; Palmqvist, E.; Hahn-Hägerdal, B.; Tengborg, C.; Stenberg, K.; Zacchi, G.; Nilvebrant, N.O. The generation of fermentation inhibitors during dilute acid hydrolysis of softwood. *Enzym. Microb. Technol.* **1999**, *24*, 151–159. [CrossRef]
17. Cuthbert, R.; Taggart, M.A.; Prakash, V.; Saini, M.; Swarup, D.; Upreti, S.; Mateo, R.; Chakraborty, S.S.; Deori, P.; Green, R.E. Effectiveness of action in India to reduce exposure of Gyps vultures to the toxic veterinary drug diclofenac. *PLoS ONE* **2011**, *6*, e19069. [CrossRef]
18. Rzymski, P.; Drewek, A.; Klimaszyk, P.J.L.R. Pharmaceutical pollution of aquatic environment: An emerging and enormous challenge. *Limnol. Rev.* **2017**, *17*, 97. [CrossRef]
19. Jiang, J.-Q. The role of coagulation in water treatment. *Curr. Opin. Chem. Eng.* **2015**, *8*, 36–44. [CrossRef]
20. Teh, C.Y.; Budiman, P.M.; Shak, K.P.; Wu, T.Y. Recent advancement of coagulation–flocculation and its application in wastewater treatment. *Ind. Eng. Chem. Res.* **2016**, *55*, 4363–4389. [CrossRef]
21. Nicholas, P.C.; Cheremisinoff, A. *Handbook of Water and Wastewater Treatment Technologies*; Butterworth-Heinemann: Oxford, UK, 2002.
22. Ratnayaka, D.D.; Brandt, M.J.; Johnson, M. *Water Supply*; Butterworth-Heinemann: Oxford, UK, 2009.
23. Gray, N. *Water Technology*; CRC Press: Boca Raton, FL, USA, 2017.
24. Salih, M.; Abdulkhair, B.Y.; Alotaibi, M. Insight into the Adsorption Behavior of Carbon Nanoparticles Derived from Coffee Skin Waste for Remediating Water Contaminated with Pharmaceutical Ingredients. *Chemistry* **2023**, *5*, 1870–1881. [CrossRef]
25. Hucknall, A.; Rangarajan, S.; Chilkoti, A. In pursuit of zero: Polymer brushes that resist the adsorption of proteins. *Adv. Mater.* **2009**, *21*, 2441–2446. [CrossRef]
26. Rasheed, T.; Ahmad, N.; Ali, J.; Hassan, A.A.; Sher, F.; Rizwan, K.; Iqbal, H.M.; Bilal, M. Nano and micro architectured cues as smart materials to mitigate recalcitrant pharmaceutical pollutants from wastewater. *Chemosphere* **2021**, *274*, 129785. [CrossRef] [PubMed]
27. Cai, Y.; Chen, Z.; Wang, S.; Chen, J.; Hu, B.; Shen, C.; Wang, X. Carbon-based nanocomposites for the elimination of inorganic and organic pollutants through sorption and catalysis strategies. *Sep. Purif. Technol.* **2023**, *308*, 122862. [CrossRef]
28. Liu, Z.; Ling, Q.; Cai, Y.; Xu, L.; Su, J.; Yu, K.; Wu, X.; Xu, J.; Hu, B.; Wang, X. Synthesis of carbon-based nanomaterials and their application in pollution management. *Nanoscale Adv.* **2022**, *4*, 1246–1262. [CrossRef] [PubMed]
29. Almufarij, R.S.; Abdulkhair, B.Y.; Salih, M.; Alhamdan, N.M. Sweep-out of tigecycline, chlortetracycline, oxytetracycline, and doxycycline from water by carbon nanoparticles derived from tissue waste. *Nanomaterials* **2022**, *12*, 3617. [CrossRef] [PubMed]
30. Jjagwe, J.; Olupot, P.W.; Menya, E.; Kalibbala, H.M. Synthesis and application of Granular activated carbon from biomass waste materials for water treatment: A review. *J. Bioresour. Bioprod.* **2021**, *6*, 292–322. [CrossRef]
31. Kan, Y.; Zhang, R.; Xu, X.; Wei, B.; Shang, Y. Comparative study of raw and HNO_3-modified porous carbon from waste printed circuit boards for sulfadiazine adsorption: Experiment and DFT study. *Chin. Chem. Lett.* **2023**, *34*, 108272. [CrossRef]
32. Kafil, M.; Nasab, S.B.; Moazed, H.; Jokiniemi, J.; Lähde, A.; Bhatnagar, A. Efficient removal of azo dyes from water with chitosan/carbon nanoflower as a novel nanocomposite synthesized by pyrolysis technique. *Desalination Water Treat.* **2019**, *142*, 308–320. [CrossRef]
33. Wan, S.; Bi, H.; Sun, L.J.N.R. Graphene and carbon-based nanomaterials as highly efficient adsorbents for oils and organic solvents. *Nanotechnol. Rev.* **2016**, *5*, 3–22. [CrossRef]
34. Tavakkoli, M.; Flahaut, E.; Peljo, P.; Sainio, J.; Davodi, F.; Lobiak, E.V.; Mustonen, K.; Kauppinen, E.I. Mesoporous single-atom-doped graphene–carbon nanotube hybrid: Synthesis and tunable electrocatalytic activity for oxygen evolution and reduction reactions. *ACS Catal.* **2020**, *10*, 4647–4658. [CrossRef]
35. Xu, W.; Dong, X.; Wang, Y.; Zheng, N.; Zheng, B.; Lin, Q.; Zhao, Y. Controllable Synthesis of MoS_2/Carbon Nanotube Hybrids with Enlarged Interlayer Spacings for Efficient Electrocatalytic Hydrogen Evolution. *ChemistrySelect* **2020**, *5*, 13603–13608. [CrossRef]
36. Fu, S.; Chen, X.; Liu, P. Preparation of CNTs/Cu composites with good electrical conductivity and excellent mechanical properties. *Mater. Sci. Eng. A* **2020**, *771*, 138656. [CrossRef]
37. Verma, B.; Goel, S.; Balomajumder, C. Multiwalled CNTs for Cr (VI) removal from industrial wastewater: An advanced study on adsorption, kinetics, thermodynamics for the comparison between the embedded and non-embedded carboxyl group. *Can. J. Chem. Eng.* **2021**, *99*, 281–293. [CrossRef]
38. Liu, G.; Su, Z.; He, D.; Lai, C. Wet ball-milling synthesis of high performance sulfur-based composite cathodes: The influences of solvents and ball-milling speed. *Electrochim. Acta* **2014**, *149*, 136–143. [CrossRef]
39. Ye, H.; Luo, Y.; Yang, T.; Xue, M.; Yin, Z. Effects of ball milling on hydrochar for integrated adsorption and photocatalysis performance. *Sep. Purif. Technol.* **2024**, *354*, 128687. [CrossRef]

40. Gao, P.; Fan, X.; Sun, D.; Zeng, G.; Wang, Q.; Wang, Q. Recent Advances in Ball-Milled Materials and Their Applications for Adsorptive Removal of Aqueous Pollutants. *Water* **2024**, *16*, 1639. [CrossRef]
41. Abdelrahman, M.M.; Naguib, I.A.; Elsayed, M.A.; Zaazaa, H.A. Spectrophotometric methods for quantitative determination of chlorhexidine gluconate and its major impurity, metabolite and degradation product: Para-chloro-aniline. *Anal. Chem. Lett.* **2016**, *6*, 232–248. [CrossRef]
42. Ibrahim, T.G.; Almufarij, R.S.; Abdulkhair, B.Y.; Ramadan, R.S.; Eltoum, M.S.; Abd Elaziz, M.E. A Thorough Examination of the Solution Conditions and the Use of Carbon Nanoparticles Made from Commercial Mesquite Charcoal as a Successful Sorbent for Water Remediation. *Nanomaterials* **2023**, *13*, 1485. [CrossRef] [PubMed]
43. Labani, M.M.; Rezaee, R.; Saeedi, A.; Al Hinai, A. Evaluation of pore size spectrum of gas shale reservoirs using low pressure nitrogen adsorption, gas expansion and mercury porosimetry: A case study from the Perth and Canning Basins, Western Australia. *J. Pet. Sci. Eng.* **2013**, *112*, 7–16. [CrossRef]
44. Thommes, M.; Kaneko, K.; Neimark, A.V.; Olivier, J.P.; Rodriguez-Reinoso, F.; Rouquerol, J.; Sing, K.S. Physisorption of gases, with special reference to the evaluation of surface area and pore size distribution (IUPAC Technical Report). *Pure Appl. Chem.* **2015**, *87*, 1051–1069. [CrossRef]
45. Sun, S.; Liang, F.; Tang, L.; Wu, J.; Ma, C. Microstructural investigation of gas shale in Longmaxi formation, Lower Silurian, NE Sichuan basin, China. *Energy Explor. Exploit.* **2017**, *35*, 406–429. [CrossRef]
46. Elamin, M.R.; Abdulkhair, B.Y.; Elzupir, A.O. Removal of ciprofloxacin and indigo carmine from water by carbon nanotubes fabricated from a low-cost precursor: Solution parameters and recyclability. *Ain Shams Eng. J.* **2023**, *14*, 101844. [CrossRef]
47. Abdulkhair, B.Y.; Elamin, M.R. Low-cost carbon nanoparticles for removing hazardous organic pollutants from water: Complete remediation study and multi-use investigation. *Inorganics* **2022**, *10*, 136. [CrossRef]
48. Supriya, S.; Sriram, G.; Ngaini, Z.; Kavitha, C.; Kurkuri, M.; De Padova, I.P.; Hegde, G. The role of temperature on physical–chemical properties of green synthesized porous carbon nanoparticles. *Waste Biomass Valorization* **2020**, *11*, 3821–3831. [CrossRef]
49. Ayodele, O.; Olusegun, S.J.; Oluwasina, O.O.; Okoronkwo, E.A.; Olanipekun, E.O.; Mohallem, N.D.; Guimarães, W.G.; Gomes, B.L.D.M.; Souza, G.D.O.; Duarte, H.A. Experimental and theoretical studies of the adsorption of Cu and Ni ions from wastewater by hydroxyapatite derived from eggshells. *Environ. Nanotechnol. Monit. Manag.* **2021**, *15*, 100439. [CrossRef]
50. Elamin, M.R.; Ibnaouf, K.H.; Elamin, N.Y.; Adam, F.A.; Alolayan, A.H.; Abdulkhair, B.Y. Spontaneous Adsorption and Efficient Photodegradation of Indigo Carmine under Visible Light by Bismuth Oxyiodide Nanoparticles Fabricated Entirely at Room Temperature. *Inorganics* **2022**, *10*, 65. [CrossRef]
51. Elamin, M.R.; Abdulkhair, B.Y.; Elzupir, A.O. Insight to aspirin sorption behavior on carbon nanotubes from aqueous solution: Thermodynamics, kinetics, influence of functionalization and solution parameters. *Sci. Rep.* **2019**, *9*, 12795. [CrossRef] [PubMed]
52. Tran, H.N.; You, S.J.; Hosseini-Bandegharaei, A.; Chao, H.P. Mistakes and inconsistencies regarding adsorption of contaminants from aqueous solutions: A critical review. *Water Res.* **2017**, *120*, 88–116. [CrossRef]
53. Adam, F.A.; Ghoniem, M.G.; Diawara, M.; Rahali, S.; Abdulkhair, B.Y.; Elamin, M.R.; Aissa, M.A.B.; Seydou, M. Enhanced adsorptive removal of indigo carmine dye by bismuth oxide doped MgO based adsorbents from aqueous solution: Equilibrium, kinetic and computational studies. *RSC Adv.* **2022**, *12*, 24786–24803. [CrossRef] [PubMed]
54. Almufarij, R.S.; Abdulkhair, B.Y.; Salih, M.; Aldosari, H.; Aldayel, N.W. Optimization, nature, and mechanism investigations for the adsorption of ciprofloxacin and malachite green onto carbon nanoparticles derived from low-cost precursor via a green route. *Molecules* **2022**, *27*, 4577. [CrossRef] [PubMed]
55. Alrobei, H.; Prashanth, M.K.; Manjunatha, C.R.; Kumar, C.P.; Chitrabanu, C.P.; Shivaramu, P.D.; Kumar, K.Y.; Raghu, M.S. Adsorption of anionic dye on eco-friendly synthesised reduced graphene oxide anchored with lanthanum aluminate: Isotherms, kinetics and statistical error analysis. *Ceram. Int.* **2021**, *47*, 10322–10331. [CrossRef]
56. Elamin, M.R.; Abdulkhair, B.Y.; Algethami, F.K.; Khezami, L. Linear and nonlinear investigations for the adsorption of paracetamol and metformin from water on acid-treated clay. *Sci. Rep.* **2021**, *11*, 13606. [CrossRef]